The orientation of Listing's Plane in microgravity

Andrew H. Clarke [a,*], Thomas Haslwanter [b]

[a] *Charité Medical School, Berlin, FRG*
[b] *University of Applied Sciences, Linz, Austria*

Abstract

The orientation of Listing's Plane (LP) was examined under one-g and zero-g conditions during parabolic flight. Ten healthy subjects participated in the experiment. In zero-g the orientation of LP was consistently altered. LP elevation was tilted backwards by approx. 10° ($p = 0.003$). The azimuth angles of the left and right eyes also diverged in zero-g, with a statistically significant change ($p = 0.04$) in the vergence angle between 6.1° and 11.8°. A discernible dissociation in torsional eye position was also observed, which proved to be statistically significant ($p = 0.03$). The thickness of LP was found to be of the order of 1°, and was not significantly altered by the transitions between one-g and zero-g. Additional control experiments involving repeated measurements of LP under normal laboratory conditions demonstrated that the parameters of LP remain stable in the individual.

The parabolic flight results demonstrate that in contrast to re-orientation in the one-g gravitational field, the elimination of gravity represents a qualitative change for the vestibular and oculomotor systems. It appears that given the lack of voluntary control of ocular torsion, the tonic otolith afferences are instrumental in the stabilisation of torsional eye position and consequently of Listing's Plane. The observed torsional divergence also provides support for the so-called otolith asymmetry hypothesis.
© 2007 Elsevier Ltd. All rights reserved.

Keywords: Listing's plane; Gravity; Microgravity; Otolith; Eye movements; Video-oculography

1. Introduction

Since the late 19th century (e.g., (Helmholtz, 1867)), it has been known that under normal visual conditions with the head in the comfortable upright position, the torsional orientation of the eye is independent of the path that the eye takes to reach any secondary or tertiary eye position. This restriction implies a reduction from three to two degrees of freedom for the eyeball, and is known as "Donders' Law". The precise behaviour of ocular torsion is specified by "Listing's Law", which states that all axes about which the eye rotates from the so-called "primary position" lie in one plane, in "Listing's Plane"; this can be visualised by representing 3D eye positions as quaternions (Tweed & Vilis, 1987) or rotation vectors (Haustein, 1989). It has been shown that Listing's law holds during fixations, saccades and smooth pursuit (Straumann, Zee, Solomon, & Kramer, 1996), and it has been argued that Listing's plane is primarily under visuomotor control (Hepp et al., 1997). Nevertheless, under one-g conditions the orientation of Listing's plane in the monkey has been found to be dependent on the head's orientation to gravity (Haslwanter, Straumann, Hess, & Henn, 1992). However this proves to be much less in the human (Bockisch & Haslwanter, 2001; Furman & Schor, 2003). In a detailed analysis of vestibular evoked eye movements, Hess & Angelaki have also demonstrated that under dynamic re-orientations with respect to gravity, the orientation of LPs in monkeys depends strongly on head orientation (Hess & Angelaki, 1997a, 1997b). These changes in the elevation of LP should not be confused with the well-documented occurrence of ocular counterrolling (OCR) when the head is tilted to

---

* Corresponding author. Address: HNO Forschung, Charité Campus Benjamin Franklin, Hindenburgdamm 30, 12200 Berlin, Germany.
  E-mail address: andrew.clarke@charite.de (A.H. Clarke).

the right or left under one-g conditions (Diamond & Markham, 1983), which manifests as a translation of LP along the naso-occipital (x-) axis of the head.

Previous investigations of the effects of microgravity on the three-dimensional vestibulo-ocular reflex (3D VOR) demonstrate that the loss of the otolith-mediated gravity vector leads to a gain reduction of the torsional component, and thus to a re-orientation of its coordinate frame over the course of long-duration stays in microgravity.

The present study examines the behaviour of LP in the one-g and zero-g phases of parabolic flight. This permits investigation of the short-term effects of the absence of gravity on the orientation of LP, i.e., of its dependence on the otolith-mediated gravito-inertial vector.

2. Methods

The main experiment was performed onboard the Airbus parabolic flight aircraft (Novespace, Bordeaux, F). Twelve healthy subjects (male, aged between 27 and 54) participated, who had passed a standard flight medical test. The parabolic flight profile consisted of a period of 2 min straight-and-level flight – providing a baseline, one-g condition. This was followed by a "pull-up phase" of approximately 30 s, during which the gravito-inertial level increased to approximately 1.8 g. The subsequent free-fall or zero-g phase lasted approximately 25 s. This was followed by a so-called "pull-out phase", again with increased g-level of up to 1.8 g. throughout the experiment each subject was seated on the floor of the aircraft facing forward in the direction of flight in alignment with the fore-aft axis, as depicted by the cartoons on the left of Fig. 3. The trunk and head were held upright, supported by foam padding. Subjects were instructed to hold the head still in a comfortable upright position during the trials. Control experiments were also conducted in the laboratory to establish the intraindividual variability of LP.

All measurements and evaluation of eye and head movements were performed with a binocular, three-dimensional eye tracking device (ETD, Chronos Vision, Berlin). A detailed description of this device has been published previously (Clarke, Steineke, & Emanuel, 2000). In summary, the eye tracker provides for binocular measurement of 3D eye position with an angular resolution of <0.1°. In the present study recording was performed with a sampling rate of 100 Hz. Inertial tri-axial angular rate sensors and linear accelerometers mounted on the head unit of the ETD permit simultaneous recording of head rotation and translation. Throughout the trials, the analogue sensor signals were sampled and digitised (16 bit) synchronously with the frame rate (100 Hz) of the images of the eye tracker, and each set of sampled values stored on hard disk together with the corresponding image frame. These sensor data were evaluated to provide a quantitative measure of head movement during the experiment trials.

Device slippage relative to the head was minimised by using customised thermoplastic facemasks for each subject. These were locked to the head unit and were worn throughout the measurements.

Calibration of eye movements was performed by evaluation of a sequence of fixations to target spots set at fixed angles. The targets were generated using a laser diode fitted with a diffraction grating and attached to the centre of the visor of the head-mounted eye tracker. This provided a 3×3 matrix of red spots at fixed angles (+9° horizontal & vertical) in the subject's frontal plane that remained constant regardless of any changes in head position. The calibration procedure was repeated during each straight-and-level phase of the flight before each parabola manoeuvre. During the consecutive one-g and zero-g phases the subject was instructed to perform sequences of random saccades for a period of 20 s. To assist this task, a target board with an array of randomly spaced target points within a horizontal and vertical range of ±20° was mounted at a distance of 2 m, in the subject's frontal plane. Each subject was measured during the course of four to eight successive parabolae.

The recorded eye image sequences were analysed offline after completion of the flights. The image processing techniques employed have been described previously Clarke, Ditterich, Druen, Schonfeld, & Steineke, 2002 and draw largely from the approaches by Hatamian & Anderson (Hatamian & Anderson, 1983) and Haslwanter & Moore (Moore, Haslwanter, Curthoys, & Smith, 1996). In summary, automatic tracking of the black pupil yields the horizontal and vertical co-ordinates of eye position. In contrast to the centre-of-gravity algorithm employed by Moore et al. (1996) a generalised Hough transform was employed for this purpose. This is considerably less sensitive to artefacts such as partial lid closure and shadowing effects. The torsional eye position was calculated by polar correlation of iris profiles, as originally described by Hatamian & Anderson (Hatamian & Anderson, 1983). Two diametrically opposite iris segments from each eye were evaluated, in order to obtain a more veridical measure of torsion (Groen, Bos, Nacken, & de Graaf, 1996). The image processing evaluation yields eye position in Euler angles, according to the Fick convention. Custom programs in Matlab (Mathworks, Inc) were used to transform the Fick coordinates into quaternions. A principal components analysis (implemented in MATLAB, Mathworks Inc.) was employed to calculate an orthogonal regression, i.e., best-fit plane to these data points. This estimate yields the elevation and azimuth angles, x-axis offset, and the thickness of LP. The thickness is defined here as +1 standard deviation of the measured eye positions about the fitted plane. With the convention introduced by Tweed, Cadera and Vilis (Tweed, Cadera, & Vilis, 1990), these planes are referred to as "displacement planes" since they are calculated relative to the current reference position. The change of the orientation of Listing's plane is twice the amount of the change of these displacement planes (Haslwanter, 1995). Data are represented in a right-handed Cartesian coordinate system, with the positive x-axis pointing forward, the y-axis to the left, and the z-axis up.

For each subject the LP parameters (elevation, azimuth, x-axis offset, thickness) were calculated for 4–6 data sets obtained from the one-g and from the zero-g phases of the parabolic flights. A sample of the eye position record employed for the calculation of LP is shown in Fig. 1. Median values were then calculated for each parameter for the subsequent statistical analysis. Initially, statistical testing for changes in elevation and thickness of LP was performed with data from all left and right eyes lumped together. For those cases where binocular data was obtained, statistics were calculated for both eyes separately and for vergence. The Wilcoxon test for matched pairs was employed. The same test was used to test LP elevation, thickness and azimuth angle for left versus right eye, and finally for the change in vergence angle (azimuth right–azimuth left) under one-g versus zero-g conditions.

Additional control measurements were performed in the laboratory with 6 subjects, using the same protocol and measurement equipment as for the flight experiment. This permitted the intra-individual variability of LP over repeated measurements to be determined. For each subject a series of 10–12 trial sessions were performed at intervals of two to three days. During each session the subject was instructed to perform sequences of random saccades for a period of 20 s. Five consecutive sequences were recorded. Monocular recording from the left eye was performed. A plane was fitted to each data sequence by orthogonal regression as described above. The standard error across the five trials in each session was calculated to assess reproducibility. The standard deviation of LP elevation and thickness across sessions was taken as a measure of the individual variability of LP for each subject overtime. The control measurements were also useful for the verification of the data obtained from the video eye tracker against previous search coil studies (Bockisch & Haslwanter, 2001; Furman & Schor, 2003).

The examination and test procedures employed were in accordance with the ethical standards of the Ethics Committee of the Charité Medical School, Berlin and the Medical Board of the European Space Agency on human experimentation and with the Declaration of Helsinki.
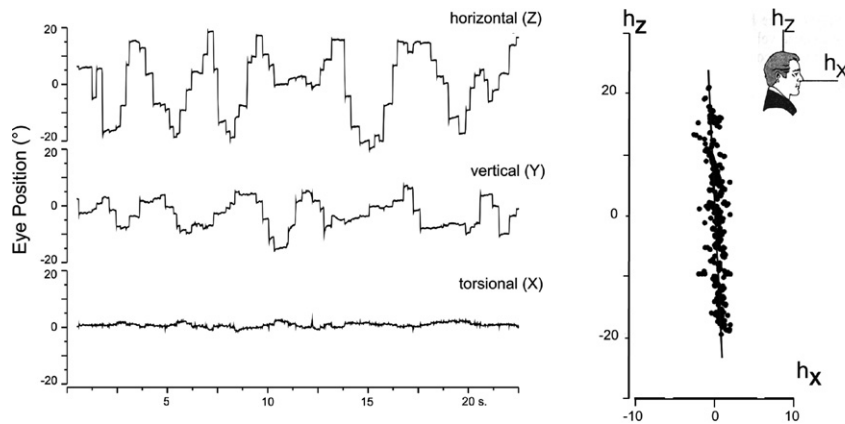
Fig. 1. Example of data recording of vertical, horizontal and torsional eye position over a sequence of fixations and saccades (left) and the corresponding X–Z projection of Listing's Plane (right).

3. Results

Of the 12 participants, 2 failed to complete the test protocol due to discomfort and airsickness. In 5 cases reliable data was obtained from both eyes. From the remaining 5 cases, useful data were obtained from one eye only, largely due to inadequate contrast in the iris landmarks of the other eye.

Control measurements in the six laboratory subjects yielded a within-session, trial-to-trial standard error of 0.9° and a day-to-day variability in the elevation of LP of 2.1°. This variability is comparable to the 3° or less, reported by van Gisbergen, Melis, and Cruysberg (1996), who determined the orientation of LP on the basis of search coil recordings. The repeat measurements also demonstrate that the thickness of LP, as derived from video eye tracker data, was consistent over subjects, with values around 1°.

The evaluation of the head movement sensor data recorded during the parabolic flights demonstrated that head movement during the measurement phases was less than 1°. Examples of three-dimensional head position traces from one-g and zero-g phases are shown in Fig. 2. The calculated RMS values of movement about the H_x, H_y and H_z axes for each of the ten subjects who completed the trials are listed in Table 1. While more head movement occurred during the zero-g phases, the range of values remained below 1° throughout the trials.

Table 1
RMS values of head position variability (in degrees), listed for each of the ten subjects who completed the inflight trials

One-g				Zero-g			
Sj No.	H_x	H_y	H_z	Sj No.	H_x	H_y	H_z
1	0.06	0.09	0.08	1	0.41	0.48	0.50
2	0.04	0.21	0.09	2	0.32	0.21	0.86
3	0.16	0.13	0.15	3	0.35	0.52	0.59
4	0.08	0.23	0.13	4	0.36	0.24	0.22
5	0.01	0.04	0.02	5	0.14	0.52	0.10
6	0.09	0.08	0.06	6	0.20	0.15	0.41
7	0.21	0.09	0.04	7	0.56	0.42	0.32
8	0.13	0.15	0.16	8	0.29	0.46	0.35
9	0.23	0.13	0.08	9	0.18	0.18	0.36
10	0.04	0.02	0.01	10	0.1	0.46	0.14
Ave	*0.11*	*0.12*	*0.08*	*Ave*	*0.29*	*0.36*	*0.39*

The RMS values were calculated over the one-g and zero-g phases of 4 consecutive parabolic flight manoeuvres. Head position variability was greater during the zero-g phases, but still remained less than 1°.
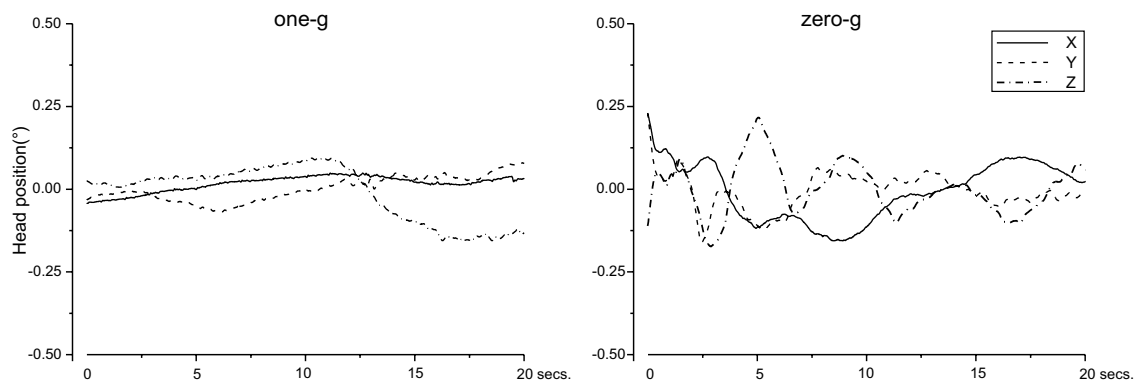

Fig. 2. Examples of head position variability during one-g and zero-g phases of parabolic flight. The three traces show the angular position of the head around the H_x, H_y and H_z axes, as measured by the headmounted sensors, over the one-g and zero-g phases.

In [Fig. 3](#) the *X–Z* projections (side view) of LP are shown for the left eye of one subject, over the one-g and zero-g phases of four successive parabolae, illustrating the consistent switching backward and forward of the angle of elevation.
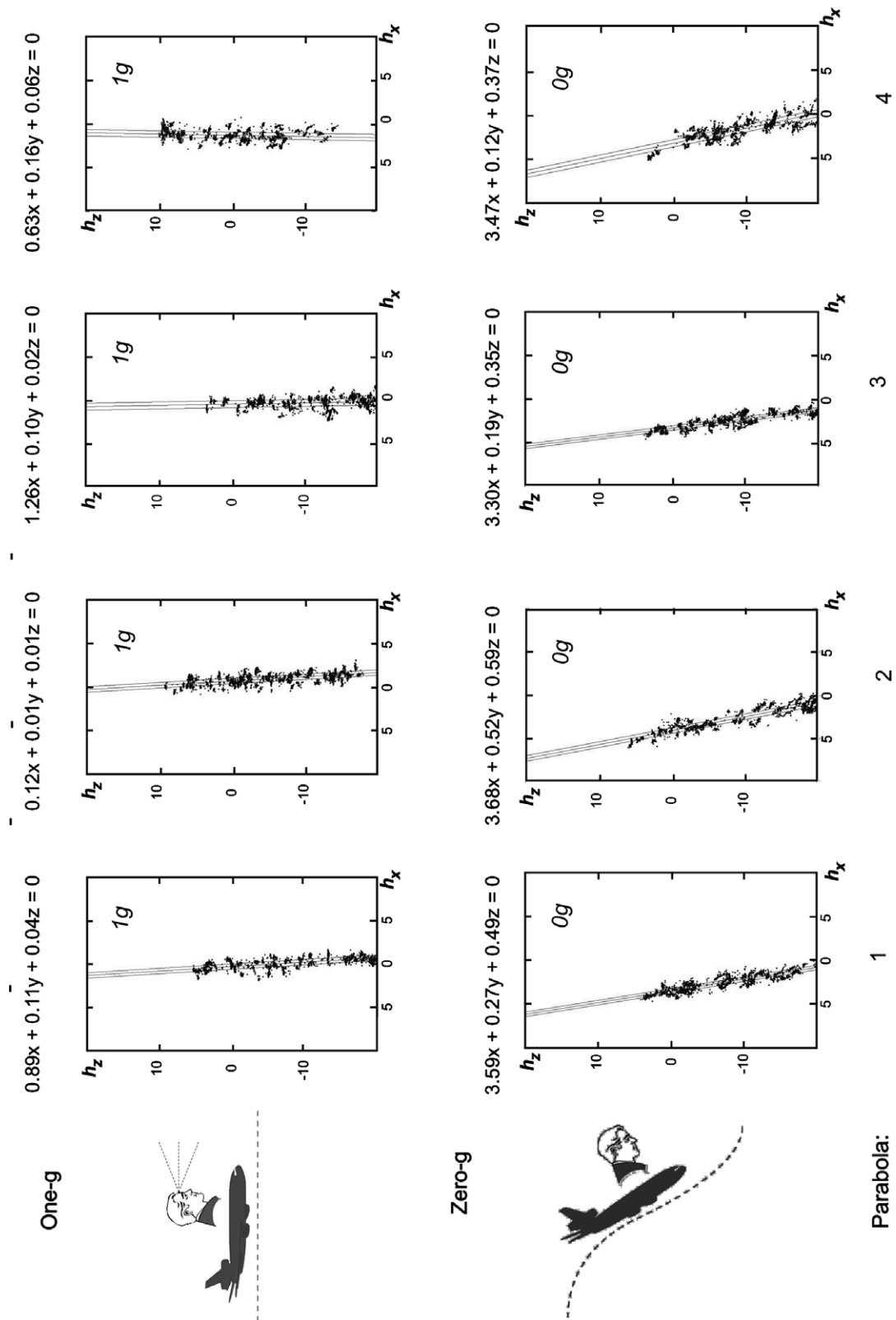

Fig. 3. *X–Z* projection of the calculated displacement planes as recorded during the one-g and zero-g phases of four consecutive parabolae, illustrating the consistent change in elevation in zero-g. The equation for each fitted plane, derived by orthogonal regression, is included. The cartoons on the left illustrate schematically the straight-and-level (1 g) and freefall (0 g) phases.

As illustrated in the example of Fig. 3, the change in elevation on transition from one-g to zero-g was consistently in one direction (tilting back). The data from the 10 subjects (15 eyes) are presented in Fig. 4a and 6a. The median change in the angle of elevation amounted to 11.2° (max 21.9°, min 3.1°). This change in orientation was found to be statistically significant (Wilcoxon matched pairs test, $p = 0.003$). For the 5 binocular data sets the median changes for the right and left eye were found to be 10.3° and 8.9°, respectively, in both cases, $p = 0.02$).

The results from the calculation of LP thickness under one-g and zero-g are presented in Fig. 4b. The median thickness in one-g amounted to 0.90° (max 1.62°, min 0.26°), and in zero-g to 0.78° (max 2.12°, min 0.32°). The thickness of LP was not found to change significantly between the one-g and zero-g intervals (Wilcoxon test for matched pairs, $p = 0.12$). The same result was found from the separate evaluation of the data from left and right eyes ($N = 5$), as shown in Fig. 6b.

Fig. 5 shows the LP projections for the left and right eyes – elevation (XZ) and azimuth (XY) – as calculated for the one-g and zero-g phases. The notable backward tilt of elevation and divergence of azimuth in the zero-g condition is consistent over all five subjects.

From these 5 binocular data sets, LP vergence was calculated from the right eye and left eye azimuth angles. The distribution of azimuth angles for the right and left eyes are shown in Fig. 6c.

The differences in left-eye azimuth angle between one-g and zero-g conditions proved to be statistically significant (Wilcoxon for matched pairs, $p = 0.04$), but this was not the case for the right eye ($p = 0.11$). Comparison of the vergence angles ($R_{azimuth} - L_{azimuth}$) between one-g and zero-g (Fig. 6d) also yielded a statistically significant difference (Wilcoxon for matched pairs, $p = 0.02$).

There is also a discernible dissociation in the torsional position of the left and right eyes, expressed as shifts along the H_x-axis. The calculated H_x-axis shifts for each eye and the corresponding torsional vergence are listed for the five

binocular data sets in Table 2. The difference in torsional vergence angles between one-g and zero-g conditions proved to be statistically significant (Wilcoxon for matched pairs, $p = 0.03$)

The 3D primary position vectors for each eye under one-g and zero-g conditions were also calculated for the 5 binocular data sets. The resultant medians for right and left eye, one-g and zero-g conditions are shown in Fig. 7. The vectors illustrate the notable reorientation of elevation and azimuth in the zero-g phases.

4. Discussion

The analysis of the parabolic flight recordings revealed a consistent gravity-dependent change in the elevation and azimuth of LP between microgravity and normal gravity. As illustrated in Figs. 3, 4, 5 and 6, a consistent re-orientation of LP was observed after transition to or from the microgravity phases of parabolic flight. This involves changes in elevation of the order of 10°, an increase in divergence between the right- and left-eye azimuth angles of LP and a small shift of LP along the x-axis, i.e., corresponding to a torsional deviation in the resting eye position. These findings indicate that transitions between one-g and zero-g induce discrete, qualitative changes in the circuitry responsible for the maintenance of LP.

The possibility that this may have been caused by head movement can be excluded, since the recorded head movements during both one-g and zero-g trials amounted to less than one degree.

Three-dimensional eye movement control is not governed by any one single parameter, but is influenced by a number of diverse requirements, such as motor efficiency (Carpenter, 1988; Tweed, 1997), monocular visual processing (Hepp, 1995), and depth vision (Schreiber, Crawford, Fetter, & Tweed, 2001). Nevertheless, it is challenging to speculate on the functional origins of the observed re-orientations of LP on transition from one-g to zero-g. The observation that the 3D orientation of LP is changed con-
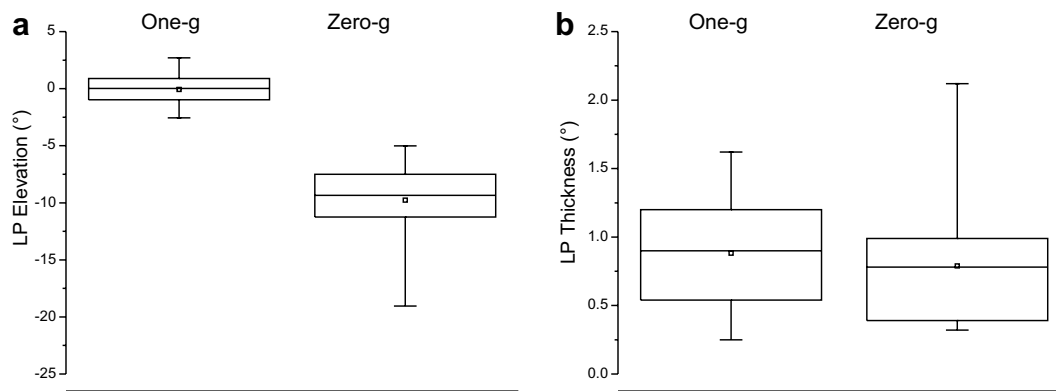

Fig. 4. Box plots of parameters calculated from all evaluated eye recordings (15 eyes), (a) LP angle of elevation (b) LP thickness, with comparison of one-g and zero-conditions. Each graph depicts the median value (horizontal bar) 25–75% range (box). 5–95% range (whiskers), and the mean value (small square).
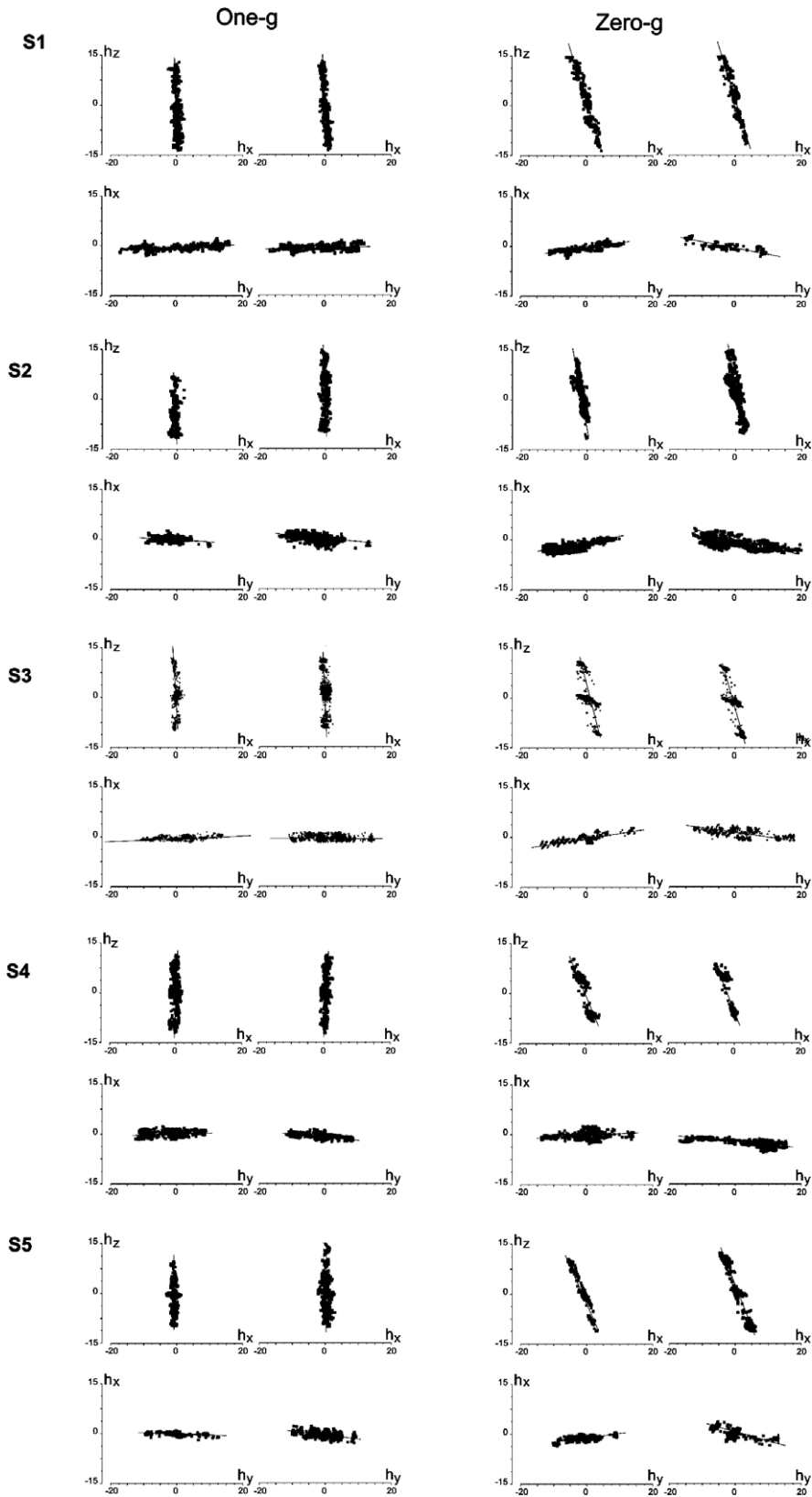
Fig. 5. Individual plots of the displacement planes for each of the five subjects evaluated binocularly. For each subject the upper plots show the elevation (H_z vs. H_x) and the lower plots the azimuth (H_x vs. H_y) for both eyes. Data for one-g (left) and for zero-g (right) conditions are included. Notable are the consistent backward tilts of the elevation and the divergence of the azimuth projections during the zero-g phases. There is also a discernible shift of LP along the X-axis in most cases – corresponding to a tonic dissociation in the torsional position of the eye (see Table 2 for values).
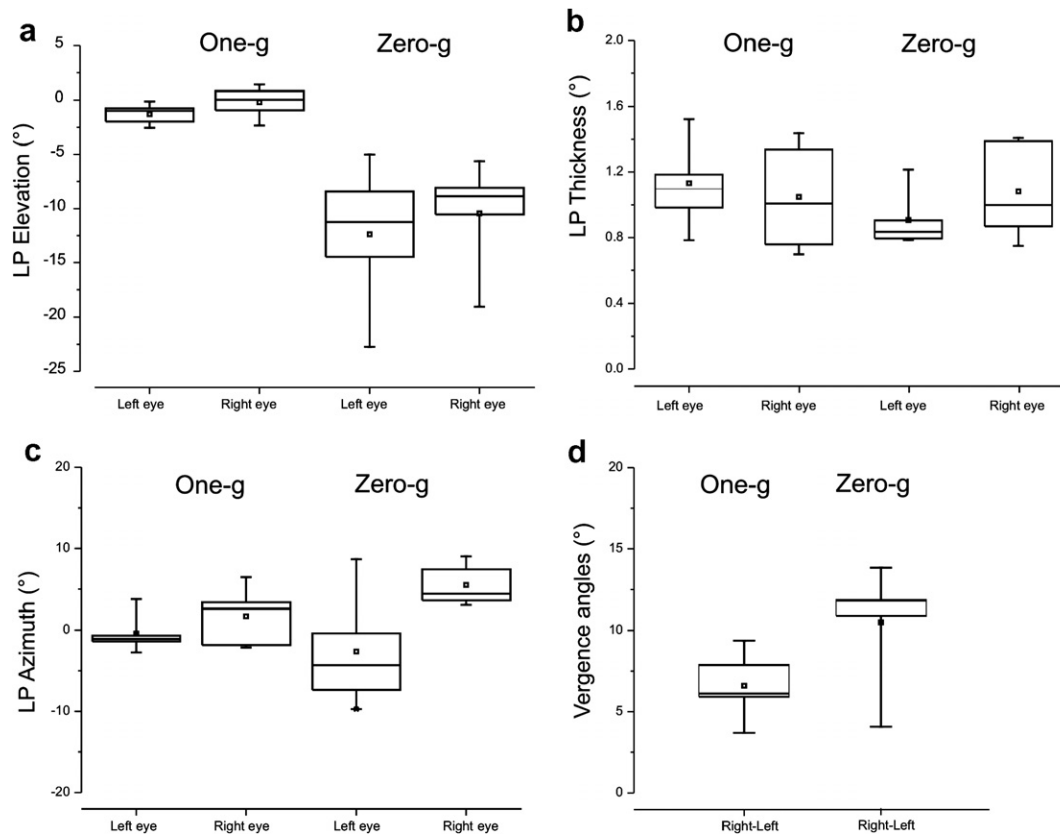
Fig. 6. Distributions of elevation, thickness, azimuth and vergence for the binocular data. Each box & whisker graph depicts the median value (horizontal bar) 25–75% range (box), 5–95% range (whiskers) and the mean value (small square). The calculated parameters are arranged for comparison of one-g and zero-g conditions. (a) LP Elevation angle for right and left eyes; (b) LP thickness for left and right eyes; (c) LP azimuth angle for each eye; and (d) LP vergence angle determined as the difference in azimuth angles of the right and left eyes.

Table 2
Deviations in the torsional position of the left (ΔT left) and right (ΔT right) eyes (specifed in degrees) and resultant change in torsional vergence (ΔT_{r-1}) after transition from one-g to zero-g conditions, listed for each of the five binocularly evaluated subjects

ΔT left (°)	ΔT right (°)	ΔT_{r-1} (°)
1	2.2	1.2
1.2	1.5	0.3
2.5	2.5	0
1	1.4	0.4
−1.25	2	3.25

sistently by these transitions strongly supports the idea that the otolith-mediated gravity reference, as propagated from the peripheral organ via the vestibular nuclei, is the driving signal for this effect. This may be interpreted in two ways.

It could be argued that LP orientation is simply modulated by the direction and magnitude of the gravito-inertial vector. This may explain the relatively small modulation of LP orientation found previously in humans during static pitch re-positioning under one-g conditions. However, it would not accommodate the very much larger changes in 3D orientation observed in the present study. At this point it is useful to note that under one-g conditions despite the
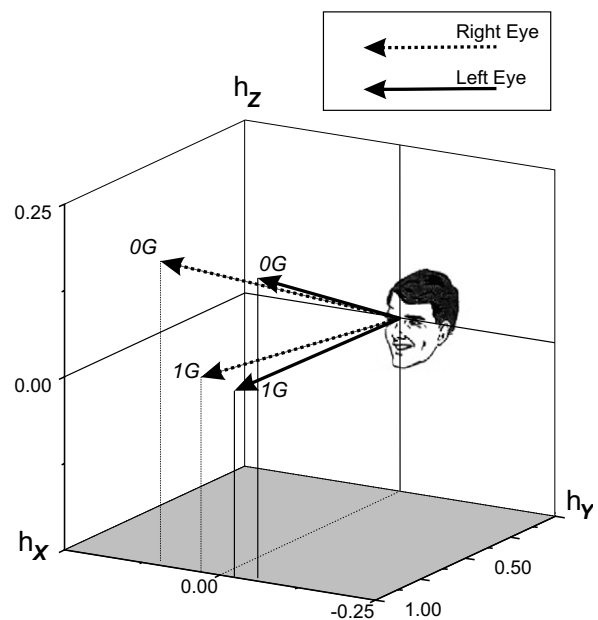

Fig. 7. Three dimensional representation of the primary position of the left and right eye during one-g and zero-g conditions during parabolic flight. Each vector depicts the median value calculated from the data of five subjects. The tilt in LP elevation and the divergence of azimuth in zero-g conditions as quantified above is clearly visualised.

re-orientation of the head, the gravity vector remains constant, and is merely sensed from a different direction by the otolith organs. Under zero-g conditions the gravity vector is completely absent. Accordingly, the more pronounced re-orientation of LP can be understood as resulting from the radical loss of the otolith-mediated gravity reference.

This observation might be compared to the finding that changes in LP orientation occur during light sleep in monkeys (Cabungcal, Misslisch, Scherberger, Hepp, & Hess, 2001). Cabungcal et al. interpreted these findings as evidence that LP is not determined alone by the peripheral ocular plant, but rather that a coordination of central nervous processes is necessary. The present findings demonstrate that the internalised, otolith-mediated gravity reference contributes to this process. Further evidence of such a coupling between the gravity reference and the oculomotor control circuitry is the gravity dependent bias component on neural signals described by Frens, Suzuki, Scherberger, Hepp, & Henn, 1998. Based on neurophysiological data they found that while the motor layer of the superior colliculus (mSC) operates in an oculocentric coordinate system, there is also a bias in the direction of gravity. They argued that the bias modification must occur downstream of, or parallel to the mSC. In this sense the discrete change in LP orientation on transition to zero-g might be explained as the removal of such a bias component, leading to the shift or transformation of the LP coordinate frame.

The thickness of LP effectively describes the instability of the torsional component of eye movement. In the present study it was not found to differ between one-g and zero-g conditions. On first glance this appears to be contradictory to the reports by Diamond and Markham (1991), who observed an increase in the torsional component during microgravity and argued that the effect is due to the latent asymmetry in the otoconial masses. The discrepancy can be explained by the fact that their measurements were conducted under light-occluded conditions with the test subjects gazing forward into darkness, while in the present study LP thickness is determined by the amplitude of the torsional component associated with eccentric eye positions. In addition, the presence of a natural visual surround in our setup is likely to have stabilised torsional eye position.

Finally, the individual changes in ocular torsional position observed under zero-g conditions support the so-called "otolith asymmetry hypothesis" (Egorov & Samarin, 1970; von Baumgarten & Thümler, 1978), according to which any inherent otoconial mass asymmetry is centrally compensated under normal one-g conditions; however, on transition to zero-g this compensatory re-weighting would persist, and manifest as the observed deviation, or bias, in torsional eye position.

Taken together it appears that given the lack of voluntary control of ocular torsion, the tonic otolith afferences and the resultant generation of an internal gravity reference are instrumental in the stabilisation of torsional eye position, and consequently of LP. The radical loss of this gravity reference in zero-g manifests directly as the observed LP re-orientation.

Acknowledgment

References

Bockisch, C. J., & Haslwanter, T. (2001). Three-dimensional eye position during static roll and pitch in humans. *Vision Research, 41*, 2127–2137.

Cabungcal, J. H., Misslisch, H., Scherberger, H., Hepp, K., & Hess, B. J. (2001). Effect of light sleep on three-dimensional eye position in static roll and pitch. *Vision Research, 41*, 495–505.

Carpenter, R. S. (1988). *Movements of the eyes*. London: Pion Ltd.

Clarke, A. H., Steineke, C., & Emanuel, H. (2000). High image rate eye movement measurement: A novel approach using CMOS sensors and dedicated FPGA devices. In T. Lehmann (Ed.), *Bildverarbeitung in der Medizin* (pp. 398–402). Berlin, New York: Springer.

Clarke, A. H., Ditterich, J., Druen, K., Schonfeld, U., & Steineke, C. (2002). Using high frame rate CMOS sensors for three-dimensional eye tracking. *Behavior Research Methods Instruments and Computers, 34*(4), 549–560.

Diamond, S. G., & Markham, C. H. (1983). Ocular counterrolling as an indicator of vestibular otolith function. *Neurology, 33*, 1460–1469.

Diamond, S. G., & Markham, C. H. (1991). Prediction of space motion sickness susceptibility by disconjugate eye torsion in parabolic flight. *Aviation, Space, and Environmental Medicine, 62*, 201–205.

Egorov, A. D., & Samarin, G. I. (1970). Possible change in the paired operation of the vestibular apparatus during weightlessness. *Kosmicheskaya Biologiya iAviakosmicheskaya Meditsina, 4*(2), 85–86.

Frens, M. A., Suzuki, Y., Scherberger, H., Hepp, K., & Henn, V. (1998). The collicular code of saccade direction depends on the roll orientation of the head relative to gravity. *Experimental Brain Research, 120*, 283–290.

Furman, J. M., & Schor, R. H. (2003). Orientation of Listing's plane during static tilt in young and older human subjects. *Vision Research, 43*, 67–76.

Groen, E., Bos, J. E., Nacken, P. F., & de Graaf, B. (1996). Determination of ocular torsion by means of automatic pattern recognition. *IEEE Transaction on Biomedical Engineering, 43*, 471–479.

Haslwanter, T., Straumann, D., Hess, B. J., & Henn, V. (1992). Static roll and pitch in the monkey: shift and rotation of Listing's plane. *Vision Research, 32*, 1341–1348.

Haslwanter, T. (1995). Mathematics of 3-dimensional eye rotations. *Vision Research, 35*, 1727–1740.

Hatamian, M., & Anderson, D. J. (1983). Design considerations for a real-time ocular counterroll instrument. *IEEE Transaction on Biomedical Engineering, 30*, 278–288.

Haustein, W. (1989). Considerations on Listing's Law and the primary position by means of a matrix description of eye position control. *Biological Cybernetics, 60*, 411–420.

Helmholtz, H. (1867). Handbuch der physiologischen Optik. Leipzig: Voss.

Hepp, K. (1995). Oculomotor control: Listing's law and all that. *Current Opinion in Neurobiology, 4*, 862–868.

Hepp, K., van Opstal, A. J., Suzuki, Y., Straumann, D., Hess, B. J. M., & Henn, V. (1997). Listing's law: Visual, motor, or visuomotor? In M. Fetter, T. Haslwanter, H. Misslisch, & D. Tweed (Eds.), *Three-dimensional kinematics of eye, head and limb movements* (pp. 33–42). Harwood academic publishers.

Hess, B. J., & Angelaki, D. E. (1997a). Kinematic principles of primate rotational vestibulo-ocular reflex. I. Spatial organization of fast phase velocity axes. *Journal of Neurophysiology, 78*, 2193–2202.

Hess, B. J., & Angelaki, D. E. (1997b). Kinematic principles of primate rotational vestibulo-ocular reflex. II. Gravity-dependent modulation of primary eye position. *Journal of Neurophysiology, 78*, 2203–2216.

Moore, S. T., Haslwanter, T., Curthoys, I. S., & Smith, S. T. (1996). A geometric basis for measurement of three-dimensional eye position using image processing. *Vision Research, 36*, 445–459.

Schreiber, K., Crawford, J. D., Fetter, M., & Tweed, D. (2001). The motor side of depth vision. *Nature, 410*, 819–822.

Straumann, D., Zee, D., Solomon, D., & Kramer, P. D. (1996). Validity of Listing's law during fixations, saccades, smooth pursuit eye movements, and blinks. *Experimental Brain Research, 112*, 135–146.

Tweed, D. (1997). Visual-motor optimization in binocular control. *Vision Research, 37*, 1939–1951.

Tweed, D., Cadera, W., & Vilis, T. (1990). Computing three-dimensional eye position quaternions and eye velocity from search coil signals. *Vision Research, 30*, 97–110.

Tweed, D., & Vilis, T. (1987). Implications of rotational kinematics for the oculomotor system in three dimensions. *Journal of Neurophysiology, 58*, 832–849.

van Gisbergen, J. A. M., Melis, B. J. M., & Cruysberg, J. R. M. (1996). Effects of alternating fixation on the binocular alignment of Listing's plane. In M. Fetter, T. Haslwanter, H. Misslich, & D. Tweed (Eds.), *Three-dimensional kinematics of eye head and limb movements.* Amsterdam: Harwood Academic.

von Baumgarten, R. J., & Thümler, R. A. (1978). A model for vestibular function in altered gravitational states. *Life Science Space Research, 17*, 161–170.